Biosensors and Bioelectronics 25 (2010) 1809–1815

Contents lists available at ScienceDirect

Biosensors and Bioelectronics

journal homepage: www.elsevier.com/locate/bios

Electrical interfacing between neurons and electronics via vertically integrated sub-4 μm-diameter silicon probe arrays fabricated by vapor–liquid–solid growth

Takeshi Kawano[a,*], Tetsuhiro Harimoto[a,c], Akito Ishihara[c], Kuniharu Takei[a], Takahiro Kawashima[b], Shiro Usui[d], Makoto Ishida[a]

[a] Department of Electrical and Electronic Engineering, Toyohashi University of Technology, 1-1 Tempaku-cho, Toyohashi, Aichi 441-8580, Japan
[b] Department of Production Systems Engineering, Toyohashi University of Technology, 1-1 Tempaku-cho, Toyohashi, Aichi 441-8580, Japan
[c] School of Life System Science and Technology, Chukyo University, 101 Tokodachi, Kaizu-cho, Toyota, Aichi 470-0393, Japan
[d] Neuroinformatics Lab., RIKEN BSI, 2-1 Hirosawa, Wako, Saitama 351-0198, Japan

ARTICLE INFO

Article history:
Received 2 October 2009
Received in revised form
10 December 2009
Accepted 31 December 2009
Available online 6 January 2010

Keywords:
Neural interface
Microelectrode array
Vapor–liquid–solid growth
Integrated circuit (IC)
MOSFET
Retina

ABSTRACT

We report here a technique for use in electrical interfaces between neurons and microelectronics, using vertically integrated silicon probe arrays with diameters of 2–3.5 μm and lengths of 60–120 μm. Silicon probe arrays can be fabricated by selective vapor–liquid–solid (VLS) growth. A doped n-type silicon probe with the resistance of 1 kΩ has an electrical impedance of less than 10 MΩ in physiological saline. After inserting the probe arrays into the retina of a carp (*Cyrpinus carpio*), we conducted electrical recording of neural signals, using the probes to measure light-evoked electrical neural signals. We determined that recorded signals represented local field potentials of the retina (electroretinogram (ERG)). The VLS-probe can provide minimally invasive neural recording/stimulation capabilities at high spatial resolution for fundamental studies of nervous systems. In addition, the probe arrays can be integrated with microelectronics; therefore, these probes make it possible to construct interfaces between neurons and microelectronics in advanced neuroscience applications.

1. Introduction

For many years, neurophysiologists have investigated nervous systems via electrophysiological measurement, using small electrodes such as glass capillaries and metal wires. Starting in the 1970s, the technology of the electrode has rapidly improved, assisted by advances in microfabrication technology. These advances have facilitated the development of microelectrode arrays, ranging from three-dimensional (3D) silicon-based penetrating probes to flexible probes (Wise and Najafi, 1991; Bai and Wise, 2001; Jones et al., 1992; Rousche et al., 2001; Takeuchi et al., 2005). Such arrays allow simultaneous recording and/or stimulation of a large number of neurons in a tissue. Recently, the focus of neurophysiology has widened beyond fundamental studies of nervous system to include advanced technology, specifically, the implantation of microelectrodes into brain/tissue in order to create neural interfaces between cells and external devices. These technologies are intended for use in patients whose quality of life could benefit from such neural interface technology (Chapin et al., 1999; Wessberg et al., 2000; Hochberg et al., 2006; Kringelbach et al., 2007).

Previous research has resulted in the development of microelectrodes; at present, several types of electrodes are commercially available. Although these electrodes have opened up new fields within neuroscience, the fabrication techniques are still under development. Some of these techniques present major challenges, e.g., minimization of probe size in order to decrease the invasiveness of electrode penetration. Conventional fabrication technologies can only achieve a probe diameter of the scale of tens of microns (μm), e.g., ~90-μm diameter at the probe base (Utah probe) (Jones et al., 1992; Hochberg et al., 2006) or ~15-μm-thick × 50-μm-wide cross-sectional area (Michigan probe) (Wise and Najafi, 1991; Bai and Wise, 2001). These dimensions are relatively large compared to the cell body of a single neuron (several microns in diameter). During electrode penetration, these probes cause damage to neurons and the surrounding tissue (Wise et al., 2004; Buzsáki, 2004), and the tissue responses associated with the damage are proportional to the probe size (Szarowski et al., 2003). Additionally, the spatial separation of larger probes is limited to the hundred-micron range, due to scaling limitations of the fabrication of the probes; these constraints result in lower spatial resolution for conventionally designed and fabricated probe arrays.

* Corresponding author. Tel.: +81 532 44 6746; fax: +81 532 44 6757.
E-mail address: kawano@eee.tut.ac.jp (T. Kawano).

0956-5663/$ – see front matter © 2010 Elsevier B.V. All rights reserved.
doi:10.1016/j.bios.2009.12.037

We can address the aforementioned electrode issues by using selective vapor–liquid–solid (VLS) growth of silicon probes (Wagner and Ellis, 1964; Ishida et al., 1999; Kawano et al., 2002). This methodology has advantages compared to the conventional fabrication techniques: it allows batch-fabrication of hundreds/thousands of probes; VLS-grown silicon probes are mechanically robust, both due to the single-crystalline nature of the silicon and the growth direction of ⟨1 1 1⟩ (Wagner and Ellis, 1964; Asai et al., 1996; Kawano et al., 2003; Takei et al., 2008; Hoffmann et al., 2006); and the probes have a smaller diameter, ranging from sub-micron to several microns, making possible the construction of high-density probe arrays (Kawano et al., 2003). We have already investigated the metallization process with high melting point metals for VLS growth as well as impurity diffusion effects due to catalytic-Au in VLS growth, confirming the compatibility of VLS-probes with the complementary metal-oxide-semiconductor (CMOS) process (Kawano et al., 2004; Kato et al., 2004; Takei et al., 2008). In this paper, we demonstrate the use of a sub-4 μm-diameter silicon probe in electrode penetrations into tissue, and electrical recordings of neural signals using a fish retina.

2. Methods and results

2.1. Integration of silicon probe arrays

Fig. 1a schematically illustrates the recording of light-evoked responses of retinal neurons, obtained using a silicon probe array. The probe arrays can be fabricated on a silicon (1 1 1) substrate by selective VLS growth using catalytic-gold (Au) dots and a disilane (Si_2H_6) gas source, allowing precise control of probe position, diameter and length, as well as on-chip interconnections/integrated circuits (ICs) (Wagner and Ellis, 1964; Ishida et al., 1999; Kawano et al., 2002) (see supplemental information (SI) text).

Fig. 1b shows a scanning electron microscope (SEM) image of a probe array designed for retinal recording. Because of the thickness of retina (~200 μm), lengths of the probes are set at 60–120 μm using a growth rate of 0.5 μm/min, at 600 °C; diameters of the probe are set at 2–3.5 μm for minimally invasive electrode penetration. Each probe is electrically conductive (heavily doped n-type silicon), and encapsulated with an insulating layer (silicon dioxide (SiO_2)), except for the recording site of the probe tip, which is

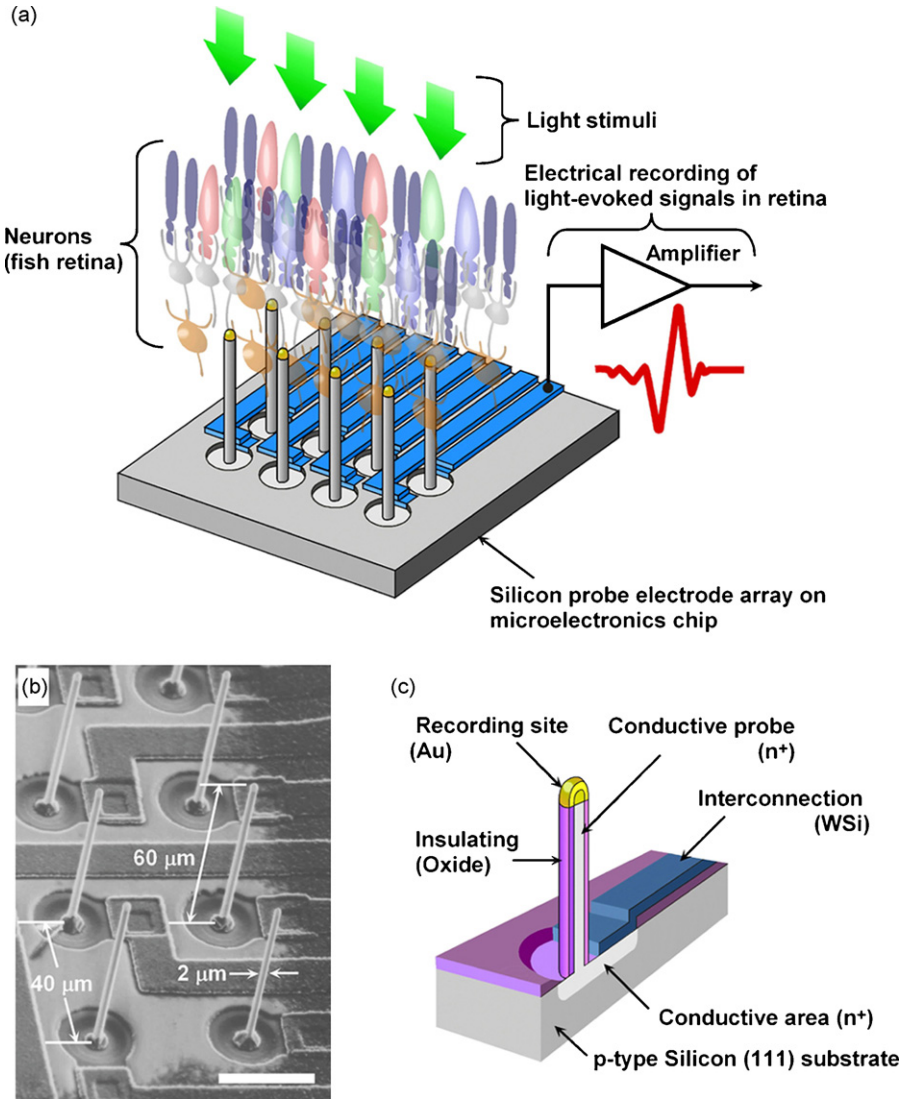

Fig. 1. Electrical neural recording with a vapor–liquid–solid grown silicon microprobes array. (a) Recording of light-evoked neural signals from retina (fish) via probes. The illumination source is placed over the retina to optically stimulate neurons (photoreceptors) in the retina. Detected electrical neural signals can be recorded through connected on-chip/off-chip amplifiers. (b) A SEM image of a 2-μm-diameter, 60-μm-length silicon probe array integrated with IC processed interconnections. Each probe site is spaced 40 μm apart. (c) A probe is composed of heavily doped n-type conductive silicon (n^+) and then covered with an insulating layer (SiO_2). The tip of the probe is formed with metal (Au) for recording of neural signals. Probes are electrically isolated by *p–n* junctions. Scale bar, 50 μm (b).

covered with metal (Au). Each probe is connected with individual interconnections (tungsten silicide (WSi))(Fig. 1c). Fig. 2a–d shows the process sequence required to integrate the probes with IC processed interconnections, as shown in Fig. 1b. Electrically conductive silicon probes can be achieved either by impurity diffusion after probe growth (phosphorus for n-type probe) (Kawano et al., 2002, 2004) or by *in situ* doping of impurities during the probe growth (PH_3 for n-type, or B_2H_6 for p-type probe) (Islam et al., 2005; Ikedo et al., 2009), resulting in resistances of 0.1–1 kΩ (Fig. 2a and b). To complete the probe processing, the sidewall of the probe is encapsulated with a 100-nm-thick SiO_2 by probe oxidation (e.g., the theoretical impedance of sidewall dioxide around a 75-μm-length, 3.5-μm-diameter probe (1 kHz) is 544 MΩ, see SI text). After the photoresist coating over the entire substrate, the probe tip region was exposed by oxygen plasma etching, and the exposed SiO_2 portion was etched by buffered hydrofluoric acid (BHF). The recording site at the probe tip is coated with biocompatible metal; here, we used 30-nm-thick Au formed by evaporation and lift-off (Fig. 2c). Because *p–n* junctions in the chip act as photodetectors (Sze, 2001), the chip itself responds to light stimuli. In order to

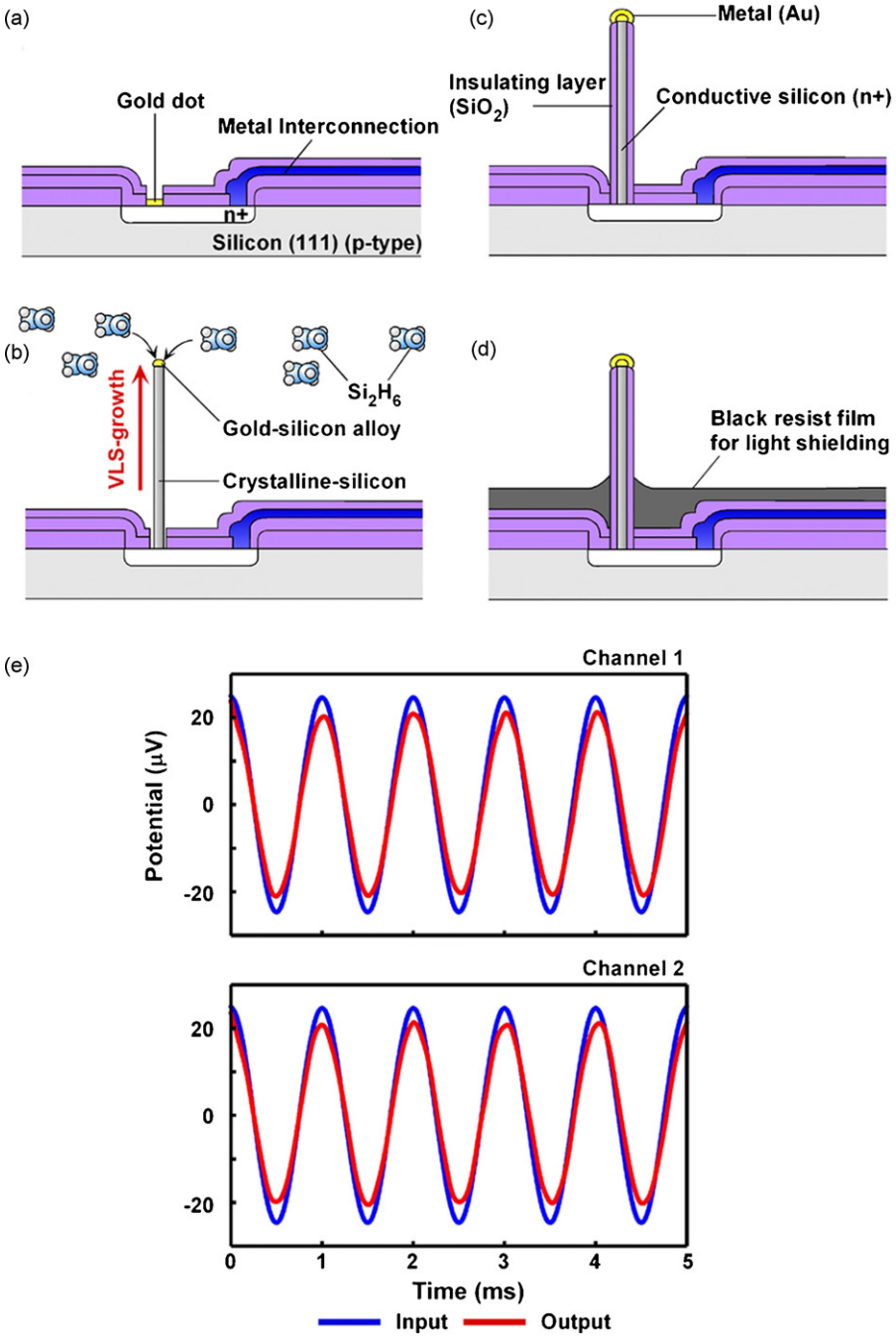

Fig. 2. Integration of silicon probe on microelectronics. (a) Vertical-aligned silicon probe grown from n-type silicon on a p-type silicon (1 1 1) substrate by selective vapor–liquid–solid growth, using catalytic Au dots and Si_2H_6 gas (b). Silicon probe electrode formed by impurity (phosphorus) diffusion process (n^+), followed by encapsulation with an insulating layer (SiO_2) and metal coating (Au) (c). A black-resist film is prepared over the substrate, in order to shield the chip from light during stimulation of the retina (d). (e) Electrical recording test of the probe in saline environment. Blue line shows sine waves (50 μV_{pp}, 1 kHz) applied to the saline, and these signals could be detected via the probes dipped in the saline (red line). These data were averaged over a period of fifty recordings (For interpretation of the references to colour in this figure legend, the reader is referred to the web version of the article.).

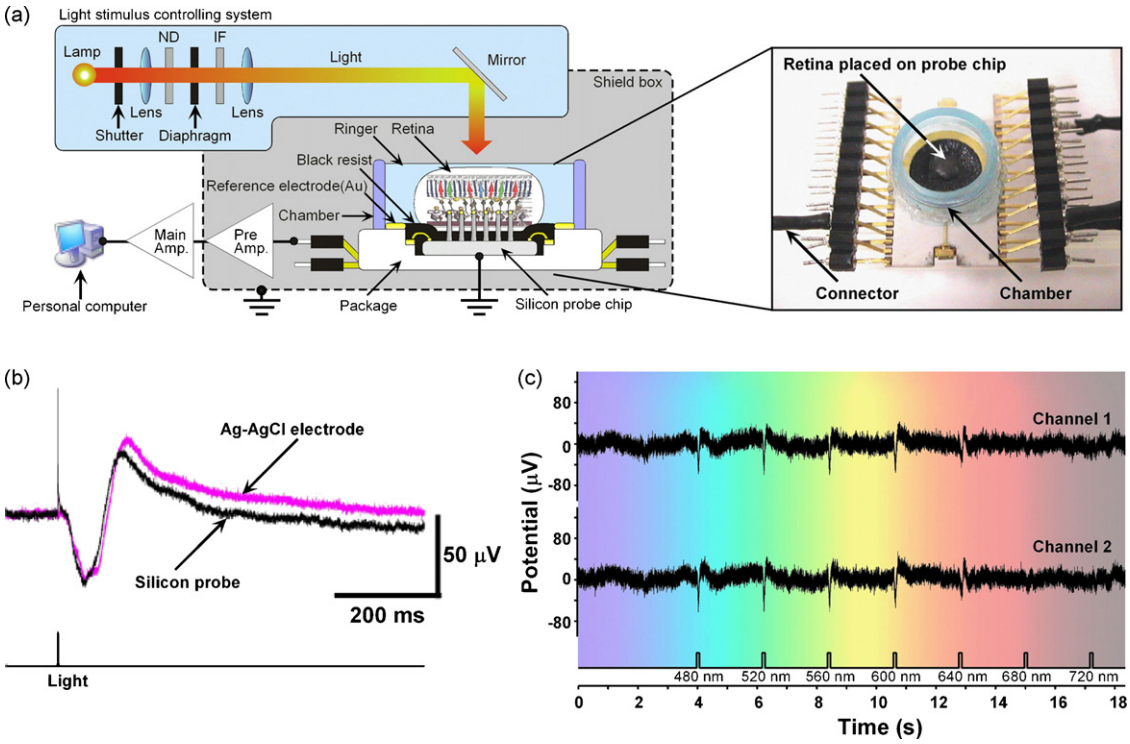

Fig. 3. Recording of light-evoked neural signals of carp retina via silicon probes. (a) Schematically illustrated experimental set-up. A fabricated chip consisting of probes is placed in a light shielded box. The isolated retina of a carp fish is placed over the chip in the recording chamber filled with carp Ringer's solution, with the probe penetration from the ganglion cell layer, as shown in the schematic diagram and the inset photograph. Light stimuli from a light-emitting diode/a light stimulus controlling system originate above the prepared retina. Detected neural signals are amplified using a preamplifier and a main amplifier, and are then stored in the personal computer. (b) Neural signals of the retina, corresponding to the light stimuli from the light emitting diode, are detected via a single silicon probe (3.5-μm-diameter, 75-μm-length). The recorded waveform is similar to another waveform recorded by a conventional Ag–AgCl electrode; we confirmed that these recorded neural signals are a typical electroretinogram (ERG) response of retinal neurons. (c) Light-evoked neural signals of the retina measured via two probes, depending on the wavelength of the light stimuli, ranging from 480 to 720 nm.

achieve light shielding, we used a 2-μm-thick black-resist film with an optical density of 3.0 (optical density = −log (per-unit transmittance) at 500-nm wavelength), which is coated over the entire chip, excluding the probes (Fig. 2d).

The electrical impedance of the probe in saline is an important determinant of the probe's utility in neural recordings (Robinson, 1968; Stieglitz, 2004). Fabricated probes with diameters of 2–3.5 μm and lengths of 75 μm, measured in saline using a ring-shaped counter electrode of a silver chloride wire (Ag–AgCl, diameter = 0.5 mm, circumferential length = 12.5 mm, impedance ≪ 1 MΩ, 1 kHz), have a probe impedance of 1–10 MΩ (1 kHz) (see SI text). The phase angle of a typical probe with an impedance of 1.1 MΩ at 1 kHz was measured to be −90° (see Fig. S1). Fig. 2e is a recording test of two probes in saline, using test sine waves with an amplitude of 50 μV_{pp}, 1 kHz, similar to extracellular signals in tissue. The signals are applied to the saline through a counter-electrode (Ag–AgCl). Even though we observed 13–21% voltage attenuation in recorded signals due to the electrical properties of the probe (see Section 3), the recording tests indicated that the VLS-microprobe can detect voltage levels similar to those of extracellular signals (<100 μV, <1 kHz).

2.2. Electrical recording of light-evoked neurons in retina

For neural recording with VLS-probes, we used the retina of a carp (*Cyrpinus carpio*). Fig. 3a shows the experimental set-up for the recording of light-evoked retinal responses; the photograph shows a device package containing a retina. The ~200-μm-thick retina was isolated from a carp (15–25 cm-length), which was dark-adapted for more than 30 min before the recording. The retina was placed on the probe chip with the ganglion cell layer facing down, where the probes were penetrated. The recording chamber was filled with carp Ringer's solution (102 mM NaCl, 2.6 mM KCl, 1.0 mM $CaCl_2$, 1.0 mM $MgCl_2$, 28 mM $NaHCO_3$, 5.0 mM glucose; buffer to pH 7.6, room temperature) (Asano, 1977). We used either a light emitting diode (LED) system or a variable-frequency light stimulation system (MVS-1, NIDEK Co., Ltd., Japan) (see SI text) mounted over the retina in order to provide light stimuli. In all retinal recordings, herein we utilized a ceramic package embedded ring-shaped Au electrode as the reference electrode (1.5 mm wide, 37 mm long, impedance ≪ 1 MΩ, 1 kHz), which surrounds the fabricated device chip (Fig. 3a). The VLS-silicon probes are mechanically robust, which had been confirmed by inserting the probe into gelatin and verifying that no probe breakdown occurred (Kawano et al., 2003; Takei et al., 2008). The silicon probes are also mechanically flexible due to the aforementioned reasons (single-crystalline nature of the silicon and the growth direction of ⟨1 1 1⟩). Such flexibility has been reported on other VLS-probes with diameters of 10–100 μm (Asai et al., 1996) or 100–200 nm (Hoffmann et al., 2006); the designed diameter of the probes in this retinal recording was 3.5 μm, with a probe length of 75 μm. These probes could be penetrated into the retina from the ganglion cell layer side. In addition, the device could be continuously used without fracturing the probe. The output leads of the chip were connected to an off-chip external high-impedance (100 MΩ) preamplifier, a main amplifier (60 dB, 0.1–10 kHz bandpass to minimize noise), and a personal computer (Fig. 3a). The background noise of the recording system without a retina was 3 μV_{rms} (rms = root-mean-square) in saline, and we considered that the inherent thermal noise at the Au-electrolyte interface to be the dominant noise source in this system (Harrison and Charles, 2003; Stieglitz, 2004).

Fig. 3b shows an example of light-evoked neural responses taken from the retina, corresponding to full-field white light stimulus from the LED (intensity = 2500 lx, duration = 50 μs). The waveform of the recorded neural response shows a transient negative amplitude of around −40 μV, which reaches its peak value at 50 ms. The negative waveform is followed by a positive waveform with a maximum amplitude of +30 μV, and it is reduced in amplitude. A spike in Fig. 3b was an artefact caused by the on/off switching of the light source; the artefact was also observed in tests without a retina. However, this artefact was observed for only 50 μs, corresponding to the light stimulation, whereas neural responses are typically delayed for several tens of milliseconds. Therefore, it was possible to separate the neural responses from the artefact. In addition to the VLS-probe device, we used another recording electrode system, a conventional Ag–AgCl electrode, mounted on a manipulator system over the retina, allowing the Ag–AgCl electrode to be in contact with another retinal surface on the photoreceptor cell layer side. The waveform of the recorded responses from the retina via the VLS-probe was simultaneously compared to responses recorded via the Ag–AgCl electrode; we found no significant difference in waveform between the two responses (Fig. 3b). These results suggest that the signals recording using the VLS-probe are indeed light-evoked neural responses of the retina. From our further characterization of recorded neural responses, we confirmed that the neural signals reflect a typical electroretinogram (ERG) response, consisting of negative *a*-waves derived from field currents produced by stimulation of photoreceptors and positive *b*-wave derived from secondary neurons postsynaptic to photoreceptors (Asano, 1977; Vann Epps et al., 2001). To confirm the locality of ERGs, we exposed the retina to slitting light stimuli, by utilizing a 1.0-mm slit between the light source and the retina. We then moved the slit laterally with a movement resolution of 500 μm and observed amplitudes of ERG as a function of slit position, indicating the local ERGs recorded (see SI text and Fig. S2). In addition, we demonstrated the spectral sensitivity of the light-evoked retinal responses (Roessel et al., 1997). Fig. 3c shows the neural responses measured by two VLS-probes during light stimuli with various wavelengths ranged from 480 to 720 nm (intensity = 4.9×10^{13} photons/cm^2/s, duration = 0.1 s). Since we used uniform light stimulation to the entire retina, we observed no significant change in the amplitude or waveform of the ERG as a function of probe position. Wavelengths in this range correspond to visible light; we observed neural responses at wavelengths of 480, 520, 560, 600 and 640 nm, and higher amplitudes were observed at 500 and 600 nm (green). A carp retina consists of two basic types of photoreceptor, rods and cones. Rods are highly sensitive photoreceptors that contain the visual pigment, rhodopsin, and are sensitive to green light with peak sensitivity, λ_{max}, around 525 nm (Kaneko and Yamada,

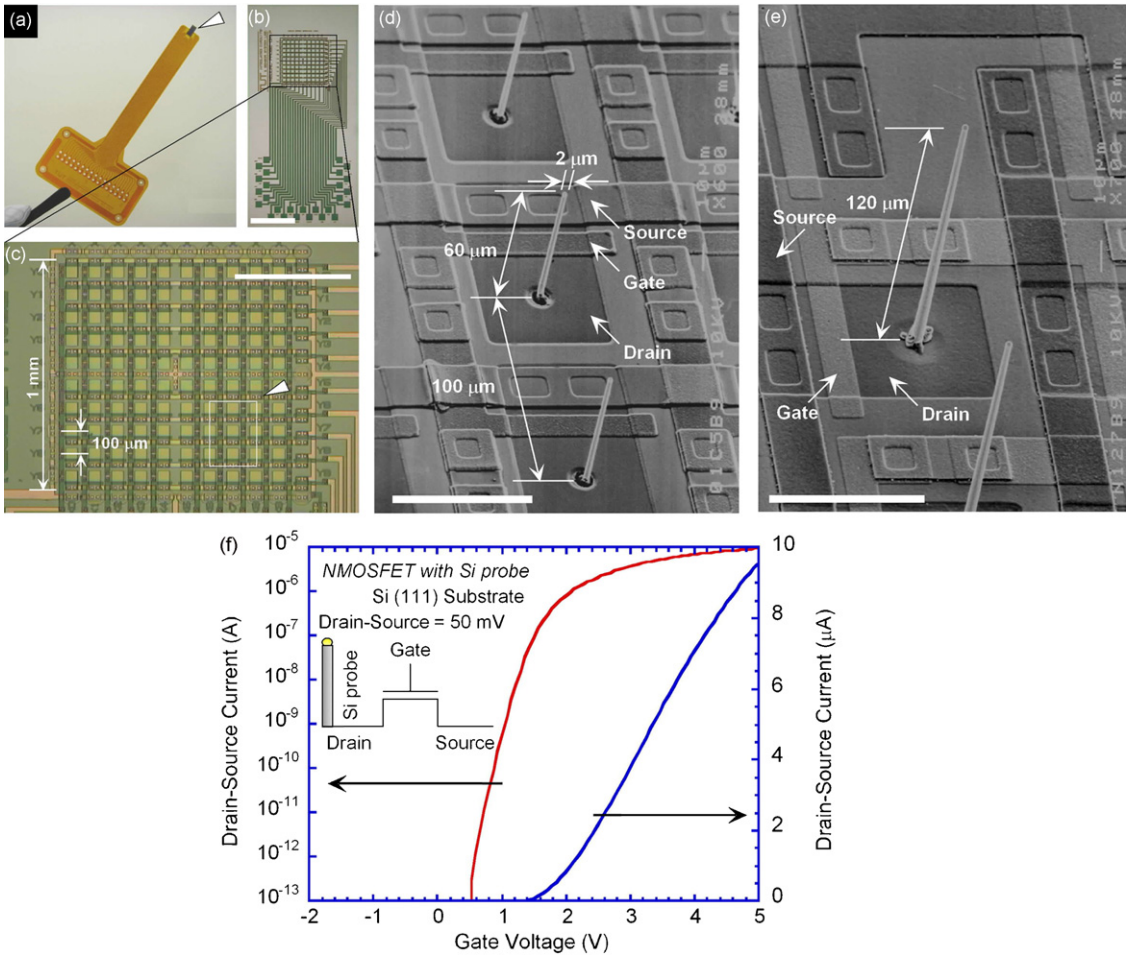

Fig. 4. Silicon probes integrated with on-chip silicon (1 1 1)-MOSFET microelectronics. A fabricated chip mounted on a flexible-polymer-based-circuitry-board (a) consists of a 10 × 10 switching array for the probe array (b). The 10 × 10 switching array is designed in a 1 mm × 1 mm recording area, and individual probes are constructed at each drain region of the MOSFET probe selector switches (c). SEM images of three 2-μm-diameter, 60-μm-length probes (d) and a 120-μm-length probe for deeper cell layer recordings (e). The MOSFET switching behavior of drain current I_D-gate voltage V_G curves for the on-chip MOSFET with probes (drain voltage = 50 mV) (f). Scale bars, 1 mm (b), 500 μm (c), 50 μm (d) and 50 μm (e).

1972; Witkovsky et al., 1973). In contrast, cones contain cone opsins, which are sensitive to either long wavelengths (red light, λ_{max} = 610 nm), medium wavelengths (green light, λ_{max} = 530 nm) or short wavelengths (blue light, λ_{max} = 460 nm). However, experimental procedure of light stimuli to the dark-adapted retina led us to conclude that the recorded higher response amplitudes at 500 and 600 nm were mainly contributed by green-sensitive rods in the carp retina. The spectral sensitivity also verified our result that detected signals were only retinal responses, without light responses associated with photodiodes (*p–n* junctions) in the chip. The fabricated device was able to be used for recording tests on 20 retinas.

2.3. On-chip microelectronics

Another advantage of this electrode technology is that the VLS-probes can be assembled directly on IC chips by fabrication of metal-oxide-semiconductor field-effect transistors (MOSFETs) on the same silicon (1 1 1) substrate (Kawano et al., 2004; Takei et al., 2008), followed by the VLS growth, similar to the process sequence shown in Fig. 2a–d. For electrically switching the selected probe element in the array during neural recording/stimulation, here we designed an on-chip site-selector circuitry using N (n-channel) MOSFET technology. Each probe was located at the drain region of the MOSFET probe selector switch, with a site spacing of 100 μm. Fig. 4a shows a probe chip mounted on a flexible-polymer-based-circuit-board used for numerous *in vivo/in vitro* neural recordings. Fig. 4b shows an optical microscopic overview of the fabricated chip; Fig. 4c shows the sensing area of the chip, consisting of a 10 × 10 array of probe sites with the site-selectors; and Fig. 4d shows a SEM image of three 2-μm-diameter, 60-μm-length probes grown at each MOSFET drain region by VLS growth, at the gas pressure of 3×10^{-3} Pa, at 600 °C, for 120 min. Fig. 4e shows another probe with a doubled length (120 μm) for use in accessing a different cell layer within the retina; this probe was fabricated using a longer VLS growth time. Impurity diffusion and encapsulation of the probes were also conducted using the same conditions described above (Fig. 2a–d). After fabricating the on-chip circuitry and probes, we characterized the device operations of the MOSFETs on silicon (1 1 1). The MOSFETs exhibited switching behavior with controlled threshold voltage and low leakage current of 10^{-12} A between the drain and the source at zero gate bias (Fig. 4f). The subthreshold swing, *S*, and field effect mobility, μ_{FE}, were 156 mV/decade and 338 cm^2/V s, respectively, and other electrical characteristics of the on-chip MOSFET on silicon (1 1 1) substrate were similar to MOSFETs on silicon (1 0 0) substrate, which were fabricated using the same MOSFET-process described here.

3. Discussion

Although the advantage of our VLS grown silicon probe is its small probe diameter (sub-4 μm), providing minimally invasive electrode penetration, the small recording area of the probe gives higher electrical impedance characteristics in saline due to the electrode–electrolyte interface and its small effective surface area (Robinson, 1968; Stieglitz, 2004). Here we assume that diameter, *d*, of the probe-tip is 2–3.5 μm (Fig. 1b) and the effective recording area is given by $2\pi(d/2)^2$ = 6.3–19.2 μm^2 (hemispherical tip shape); these values are relatively small compared to recording areas of conventional electrodes (for example, Bai and Wise (2001) shows about 100 μm^2). In this work, the recording area of VLS-probe tip was covered with Au, which has an electrical impedance in saline of 1–10 MΩ (1 kHz). In addition, the parasitic capacitances of the interconnection-saline and the interconnection-substrate cause parasitic impedances, resulting in a voltage reduction in the detected signals (Takei et al., 2008). To overcome this voltage reduction, it is necessary to reduce the electrical impedance of the probe without increasing the probe diameter. One possible way to reduce the impedance of our probe would be to use a probe tip with an enhanced surface area, achieved by introducing nanoscale roughness. Carbon nanotube-based-microelectrodes for neural recordings have been proposed (Keefer et al., 2008; Lin et al., 2009). Platinum-black sheeting, which is a biocompatible material, has been used (Regehr et al., 1989; Oka et al., 1999); we are currently exploring this platinum-black approach in our probe system (see SI text). To overcome another parasitic impedance associated with on-chip interconnections, we are working on design of on-chip preamplifier arrays, which could be fully integrated using the aforementioned IC-process (Fig. 4d and e).

A VLS-probe array with a site spacing of 40 μm has been developed. Although each probe has an individual recording site, the designed probe array's density is higher than previously reported 3D penetrating microelectrode arrays (Xu et al., 2002; Kipke et al., 2003; Vetter et al., 2004; Barthó et al., 2004; Csicsvari et al., 2003). In addition, the small diameter of the probe promises electrode insertion with only a small volume of silicon body, thus limiting the insertion tissue/neuron damage, particularly in multiple probe array penetration (Szarowski et al., 2003; Wise et al., 2004; Buzsáki, 2004). Limitations of the site spacing and the diameter of the VLS-probe depend on the aforementioned photolithography technique-based catalytic-Au patterning. Although we have designed 2–3.5 μm-diameter probes, sub-1 μm-diameter would also be achievable, providing even less invasive probe arrays. It may also be possible to design an array with a density similar to that of neurons distributed in neuronal tissue, resulting in a ratio of one neuron per individual probe during recording/stimulation. On the other hand, the VLS-probes in the array all have a same probe length, because they share the same VLS growth parameters. Therefore, these probes can only access cells in the same tissue layer. A future goal for our electrode technology is an assembly technique that allows multiple probe lengths within the same array (e.g., three types of probe lengths consisting of 50, 100 and 150 μm for the simultaneous recording of multiple layers within the fish retina). To accomplish this, we have proposed repeated selective VLS growth. Specifically, we would conduct VLS overgrowth of the primary grown silicon probes by repeated VLS growth, while the shorter probes are produced by single-step VLS growth. This technique could be applicable to construction of multiple lengths of probes in the same array (Ikedo et al., 2009).

In all device fabrications described here, silicon (1 1 1) substrate was used in order to grow VLS-probes perpendicular to the substrate. We have already developed the MOSFET circuitry process on silicon (1 1 1) substrate, and demonstrated the integration capabilities of the VLS-probe with on-chip signal processors (Kawano et al., 2004; Kato et al., 2004; Takei et al., 2008). Although all industrial ICs made with MOSFETs are fabricated on silicon (1 0 0) substrates because the SiO_2/silicon (1 0 0) interface-trap density underneath the MOSFET gate is lower than on a silicon (1 1 1) substrate (Sze, 2001), on-chip MOSFETs in our process were fabricated on silicon (1 1 1) substrates. However, the silicon (1 1 1) is an insufficient substrate in CMOS fabrication at IC-industries/foundry-services, due to the degraded properties of MOSFETs by the aforementioned issues. Furthermore, these MOSFETs suffer from mobility as well as reliability issues, particularly in cases that utilize thin-gate insulators (Momose et al., 2003). We have currently developed a heterogeneous integration of these silicon (1 1 1)-VLS-probes with silicon (1 0 0)-MOSFET circuitry; we will describe this technology in a future publication.

4. Conclusion

We described an electrode fabrication technology that can generate 2–3.5 μm-diameter silicon probe arrays using selective VLS growth, for use in various types of neural recording/stimulation experiments. The neural recording was carried out with a carp retina, and the results indicated that the VLS-probe was indeed able to detect extracellular neural signals. Give these results, and in light of the advantages of the technique (the size of probe, the high-density probe array and IC-compatibility), VLS-probe arrays could become a powerful tool for investigation of neurons both *in vivo* and *in vitro*, and could greatly assist in the study of the nervous systems. The proposed probes could be used as minimally invasive electrodes, allowing safe interfaces between neurons and neuroprosthetic devices, with applications ranging from motor control in paralysed patients to the restoration of sensory function in visual and auditory devices. This VLS-probe technique for creating interfaces between neurons and microelectronics therefore represents a significant contribution to the future of neuroscience.

Acknowledgements

We thank M. Ashiki for his assistance with the fabrication processes, A. Fujishiro for his work on platinum-black tipped VLS-probe. We are grateful for the helpful discussions of H. Kaneko at the National Institute of Advanced Industrial Science and Technology. K. Takei is a recipient of the JSPS fellowship. This work was supported in part under a grant from the Global COE Program "Frontiers of Intelligent Sensing", a Grant-in-Aid for Scientific Research (S) from the Ministry of Education, Culture, Sports, Science and Technology Japan, a CREST project of the Japan Science and Technology Agency (JST), and a Strategic Research Program for Brain Sciences (SRPBS).

Appendix A. Supplementary data

Supplementary data associated with this article can be found, in the online version, at doi:10.1016/j.bios.2009.12.037.

References

Asai, S., Kato, K., Nakazaki, N., Nakajima, Y., 1996. IEEE Transactions on Components, Packaging, and Manufacturing Technology, Part A 19, 258–267.
Asano, T., 1977. The Japanese Journal of Physiology 27, 701–716.
Barthó, P., Hirase, H., Monconduit, L., Zugaro, M., Harris, K.D., Buzsáki, G., 2004. Journal of Neurophysiology 92, 600–608.
Bai, Q., Wise, K.D., 2001. IEEE Transaction on Biomedical Engineering 48, 911–920.
Buzsáki, G., 2004. Nature Neuroscience 7, 446–451.
Chapin, J.K., Moxon, K.A., Markowitz, R.S., Nicolelis, M.A.L., 1999. Nature Neuroscience 2, 664–670.
Csicsvari, J., Henze, D.A., Jamieson, B., Harris, K.D., Sirota, A., Barthó, P., Wise, K.D., Buzsáki, G., 2003. Journal of Neurophysiology 90, 1314–1323.
Hochberg, L.R., Serruya, M.D., Friehs, G.M., Mukand, J.A., Saleh, M., Caplan, A.H., Branner, A., Chen, D., Penn, R.D., Donoghue, J.P., 2006. Nature 442, 164–171.
Hoffmann, S., Utke, I., Moser, B., Michler, J., Christiansen, S.H., Schmidt, V., Senz, S., Werner, P., Gösele, U., Ballif, C., 2006. Nano Letters 6, 622–625.
Harrison, R.R., Charles, C., 2003. IEEE Journal of Solid-State Circuits 38, 958–965.
Ikedo, A., Kawashima, T., Kawano, T., Ishida, M., 2009. Applied Physics Letters 95, 033502.
Ishida, M., Sogawa, K., Ishikawa, A., Fujii, M., 1999. Proceeding of 10th International Conference on Solid-State Sensors, Actuators and Microsystems (Transducers'99), pp. 866–869.
Islam, M.S., Ishino, H., Kawano, T., Takao, H., Sawada, K., Ishida, M., 2005. Japanese Journal of Applied Physics 44, 2161–2165.
Jones, K.E., Compbell, P.K., Normann, R.A., 1992. Annals of Biomedical Engineering 20, 423–437.
Kaneko, A., Yamada, M., 1972. Journal of Physiology 227, 261–273.
Kato, Y., Takao, H., Sawada, K., Ishida, M., 2004. Japanese Journal of Applied Physics 43, 6848–6853.
Kawano, T., Kato, Y., Futagawa, M., Tani, R., Takao, H., Sawada, K., Ishida, M., 2002. Sensors and Actuators: A, Physical 97-98, 709–715.
Kawano, T., Takao, H., Sawada, K., Ishida, M., 2003. Japanese Journal of Applied Physics 42, 2473–2477.
Kawano, T., Kato, Y., Tani, R., Takao, H., Sawada, K., Ishida, M., 2004. IEEE Transactions on Electron Devices ED-51, 415–420.
Keefer, E.W., Botterman, B.R., Romero, M.I., Rossi, A.F., Gross, G.W., 2008. Nature Nanotechnology 3, 434–439.
Kipke, D.R., Vetter, R.J., Williams, J.C., Hetke, J.F., 2003. IEEE Transaction on Neural Systems and Rehabilitation Engineering 11, 151–155.
Kringelbach, M.L., Jenkinson, N., Owen, S.L.F., Aziz, T.Z., 2007. Nature Reviews Neuroscience 8, 623–635.
Lin, C.M., Lee, Y.T., Yeh, S.R., Fang, W., 2009. Biosensors and Bioelectronics 24, 2791–2797.
Momose, H.S., Ohguro, T., Nakamura, S., Toyoshima, Y., Ishiuchi, H., Iwai, H., 2003. IEEE Transaction on Electron Devices 49, 1597–1605.
Oka, H., Shimono, K., Ogawa, R., Sugihara, H., Taketani, M., 1999. Journal of Neuroscience Methods 93, 61–67.
Regehr, W.G., Pine, J., Cohan, C.S., Mischke, M.D., Tank, D.W., 1989. Journal of Neuroscience Methods 30, 91–106.
Robinson, D.A., 1968. Proceeding of the IEEE 56, 1065–1071.
Roessel, P., Palacios, A.G., Goldsmith, T.H., 1997. Journal of Comparative Physiology A 181, 493–500.
Rousche, P.J., Pellinen, D.S., Pivin D.P.Jr., Williams, J.C., Vetter, R.J., Kipke, D.R., 2001. IEEE Transaction on Biomedical Engineering 44, 361–371.
Stieglitz, T., 2004. In: Horch, K.W., Dhillon, G.S. (Eds.), Neuroprosthetics—Theory and Practice. World Scientific.
Szarowski, D.H., Andersen, M.D., Retterer, S., Spence, A.J., Isaacson, M., Craighead, H.G., Turner, J.N., Shain, W., 2003. Brain Research 983, 23–35.
Sze, S.M., 2001. Semiconductor Devices: Physics and Technology, 2nd ed. Wiley, New York.
Takei, K., Kawashima, T., Kawano, T., Takao, H., Sawada, K., Ishida, M., 2008. Journal of Micromechanics and Microengineering 18, 035033.
Takeuchi, S., Ziegler, D., Yoshida, Y., Mabuchi, K., Suzuki, T., 2005. Lab-on-a-Chip 5, 519–523.
Vann Epps, H.A., Yim, C.M., Hurley, J.B., Brockerhoff, S.E., 2001. Investigative Ophthalmology & Visual Science 42 (3), 868–874.
Vetter, R.J., Williams, J.C., Hetke, J.F., Nunamaker, E.A., Kipke, D.R., 2004. IEEE Transaction on Biomedical Engineering 51, 896–904.
Wagner, R.S., Ellis, W.C., 1964. Applied Physics Letters 4, 89–90.
Wessberg, J., Stambaugh, C.R., Kralik, J.D., Beck, P.D., Laubach, M., Chapin, J.K., Kim, J., Biggs, S.J., Srinivasan, M.A., Nicolelis, M.A.L., 2000. Nature 408, 361–365.
Wise, K.D., Najafi, K., 1991. Science 254, 1335–1342.
Wise, K.D., Anderson, D.J., Hetke, J.F., Kipke, D.R., Najafi, K., 2004. Proceeding of the IEEE 92, 76–97.
Witkovsky, P., Nelson, J., Ripps, H., 1973. The Journal of General Physiology 61, 401–423.
Xu, C., Lemon, W., Liu, C., 2002. Sensors and Actuators: A, Physical 96, 78–85.